J Biomol NMR (2012) 52:5–10
DOI 10.1007/s10858-011-9596-z

COMMUNICATION

Simultaneous acquisition of $^{13}C^{\alpha}$–^{15}N and ^{1}H–^{15}N–^{15}N sequential correlations in proteins: application of dual receivers in 3D HNN

Swagata Chakraborty · Subhradip Paul · Ramakrishna V. Hosur

Received: 23 October 2011 / Accepted: 8 December 2011 / Published online: 28 December 2011

Abstract We describe here, adaptation of the HNN pulse sequence for multiple nuclei detection using two independent receivers by utilizing the detectable $^{13}C^{\alpha}$ transverse magnetization which was otherwise dephased out in the conventional HNN experiment. It enables acquisition of 2D $^{13}C^{\alpha}$–^{15}N sequential correlations along with the standard 3D ^{15}N–^{15}N–^{1}H correlations, which provides directionality to sequential walk in HNN, on one hand, and enhances the speed of backbone assignment, on the other. We foresee that the implementation of dual direct detection opens up new avenues for a wide variety of modifications that would further enhance the value and applications of the experiment, and enable derivation of hitherto impossible information.

Keywords $^{13}C^{\alpha}$–^{15}N correlations · Checkpoint · Dual receivers · NMR · Protein · Sequential walk

Swagata Chakraborty and Subhradip Paul contributed equally.

Electronic supplementary material The online version of this article (doi:10.1007/s10858-011-9596-z) contains supplementary material, which is available to authorized users.

S. Chakraborty · S. Paul · R. V. Hosur (✉)
Department of Chemical Sciences, Tata Institute of Fundamental Research, Homi Bhabha Road, Mumbai 400005, India
e-mail: hosur@tifr.res.in

S. Paul
Department of Chemistry, Ohio State University, 1086 Evans Laboratory, Columbus, OH 43210, USA

R. V. Hosur
UM-DAE Centre for Excellence in Basic Sciences, Mumbai University Campus, Kalina, Santa Cruz, Mumbai 400098, India

In conventional NMR experiments, only one type of nucleus is directly detected at the end of the pulse sequence and thus in multidimensional experiments, it becomes necessary to discard other detectable magnetizations that may be generated at some intermediate points of the pulse sequences. This certainly limits the information derivable from the spectra. The quest for enhancing the information content of an NMR experiment has led to the development of new hardware on the NMR spectrometers which enable direct detection of multiple nuclei simultaneously. Then, incorporation of multiple detections in the same experiment enables utilization of the otherwise discarded magnetization, thereby adding a totally new dimension to the experiment (Freeman and Kupce 2010a, b; Kupce et al. 2006, 2010; Kupce 2011; Kupce and Wrackmeyer 2010; Freeman and Kupce 2008). Such a possibility will have a great impact in protein NMR where the spectra are very complex, and their analysis typically requires several experiments to be performed to extract different and complimentary information. In this background, we demonstrate here a significant advance from the point of view of protein NMR by incorporating ^{13}C detection in addition to the usual ^{1}H detection in the HNN pulse sequence (Bhavesh et al. 2001; Panchal et al. 2001). The detectable $^{13}C^{\alpha}$ transverse magnetization which was otherwise dephased out in the conventional HNN experiment to select particular pathway is now recorded, thereby adding information from the fourth nuclear species ($^{13}C^{\alpha}$) to the 3D experiment. This implementation enables acquisition of 2D $^{13}C^{\alpha}$–^{15}N sequential correlations with some novel features, along with the standard 3D ^{15}N–^{15}N–^{1}H correlations observable in HNN, thereby creating new possibilities for rapid and unambiguous backbone assignment from a single experiment.

The modification in the HNN experiment to include dual receivers has been accomplished on a Bruker AVIII

700 MHz spectrometer equipped with two independent receivers and the new pulse sequence is depicted in Fig. 1. It begins with an INEPT transfer of magnetization from the amide proton of *i*th residue to the directly attached ^{15}N spin via the one-bond ^{1}H–^{15}N J-coupling (90–95 Hz). The transfer is followed by a constant time evolution period (30 ms) including t_1 during which the $^{15}N_i$ magnetization evolves under one (7–11 Hz) and two-bond (4–9 Hz) ^{15}N–$^{13}C^{\alpha}$ scalar couplings. At the end of this period, $^{15}N_i$ magnetization which is antiphase with respect to $^{13}C^{\alpha}$ is transferred to both self $^{13}C^{\alpha}_{i}$ and the neighboring $^{13}C^{\alpha}_{i-1}$ via a pair of 90° pulses on ^{15}N and ^{13}Cα. The transfer is followed by evolution for a period 2τ during which the $^{13}C^{\alpha}_{i}$ and $^{13}C^{\alpha}_{i-1}$ magnetizations are coupled to their own and neighboring ^{15}N spins via one-bond and two bond scalar couplings, respectively. At the end of this period, a 90°

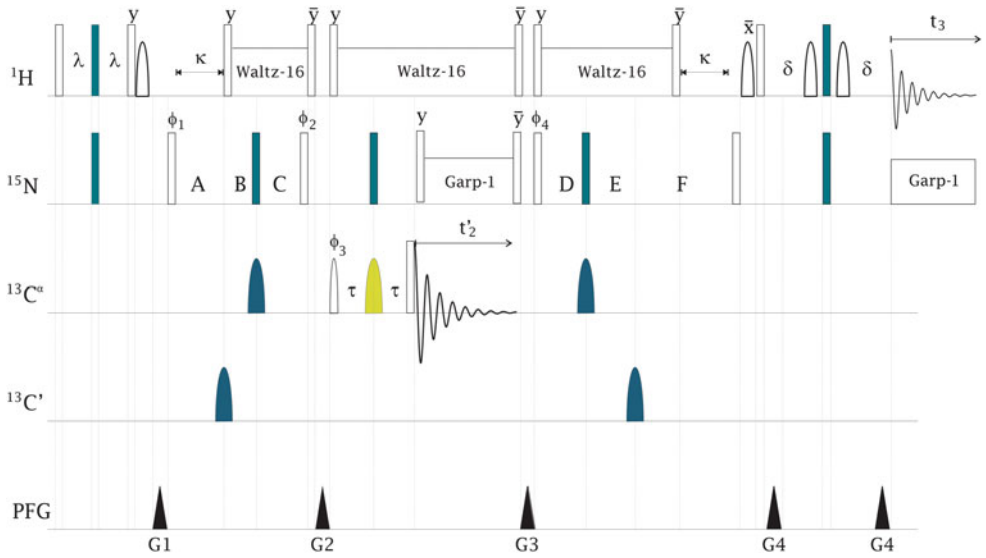

Fig. 1 Schematic diagram of the HNN pulse sequence with the incorporation of receiver 2 for $^{13}C^{\alpha}$ detection resulting in simultaneous generation of 2D ($^{13}C^{\alpha}$–^{15}N) and 3D (^{15}N–^{15}N–^{1}H) spectra. *Rectangular hollow* and *filled pulses* represent 90 and 180° hard pulses, respectively. The *filled wide pulses* and the *narrow hollow pulses* represent 180° pulses and 90° selective pulses, respectively. The ^{13}C carrier is kept at 56 ppm for effective excitation of the α-carbons. Gaussian Cascade G4 pulses [(G{270x} G{270 − x} G{270x} G{180x})] and Gaussian cascade Q3 pulses (Emsley and Bodenhausen 1990) are optimized for excitation and inversion of $^{13}C^{\alpha,\beta}$, respectively with minimal perturbation of ^{13}CO. The $^{13}C^{\alpha}_{x}$ magnetization is detected over an acquisition time of ∼20 ms which is equivalent to one GARP-1 (Shaka et al. 1985) cycle. For the ^{13}CO carbons the offset of the shaped pulses are switched to 176 ppm for minimal excitation of alpha carbons. WALTZ-16 (Shaka et al. 1983a, b) decoupling of strength 6 kHz is applied to decouple the protons from ^{15}N during both t_1 and t_2 evolutions and from C^{α} during t_2' evolution. GARP-1 decoupling of RF amplitude 1 kHz is applied during acquisition to decouple the ^{15}N from $^{13}C^{\alpha}$ during the first acquisition and from ^{1}H during the second acquisition. The delays are represented by $\lambda = 2.7$ ms, $\kappa = 5.4$ ms, and $\delta = 2.7$ ms, $A = t_1/2$, $B = T_N = 15$ ms, and $C = T_N - t_1/2$, $D = T_N - t_2/2$, $E = T_N$, $F = t_2/2$. The τ delay on the $^{13}C^{\alpha}$ channel is optimized and kept in the range of 12–16 ms. The phase cycling for the five pulses can be denoted as ϕ_1 = (x, x, −x, −x), $\phi_2 = \phi_3$ = (x, −x), ϕ_4 = (x, x, x, x, −x, −x, −x, −x) whilst the receiver 1 and receiver 2 follow phase cycling as (x, x, −x, −x, −x, −x, x, x) and (x, x, −x, −x), respectively. States-TPPI is employed on ϕ_1 and ϕ_4 to achieve frequency discrimination and pure absorption spectra (Marion et al. 1989). Sine bell shaped gradients (SINE) are used and the levels are as follows: G1 = 30% (1 ms), G2 = 30% (1 ms), G3 = 30% (1 ms) and G4 = 80% (1 ms) of the maximum gradient strength which is 53 G/cm

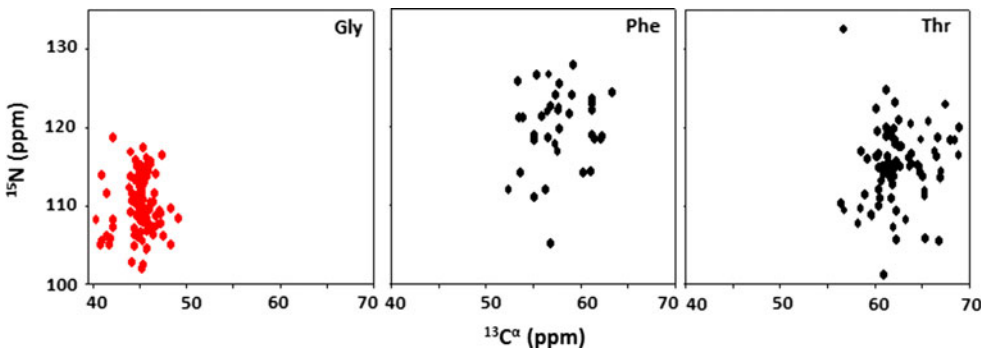

Fig. 2 2D plots of chemical shift dispersions of $^{13}C^{\alpha}$ and ^{15}N of Glycine, Phenylalanine and Threonine as obtained from BMRB accession numbers 4265, 4402, 4831, 4929, 5062, 5387, 6096, 6346, 6903, 7202, 15623 and 15743. Glycine peaks are marked with *red* to indicate negative intensities, as expected in our 2D $^{13}C^{\alpha}$–^{15}N correlation spectrum

hard pulse is applied on the ^{13}C channel (contrary to the selective pulse on $^{13}C^{\alpha}$ as in conventional HNN) to minimize relaxation loss during the pulse. At this point we are left with detectable transverse $^{13}C^{\alpha}_{i,x}$ and $^{13}C^{\alpha}_{i-1,x}$ magnetizations along with N_zC_z (which is subsequently transferred to the amide nitrogens). In the conventional HNN experiment the transverse $^{13}C^{\alpha}_{x}$ magnetizations are dephased out with the application of a gradient. However, in the double detection experiment we employ the second receiver to detect this transverse $^{13}C^{\alpha}_{x}$ magnetization while decoupling the protons and nitrogens by WALTZ-16 (Shaka et al. 1983a, b) and GARP-1(Shaka et al. 1985), respectively. The acquisition time (t_2') is optimized to be exactly equivalent to a GARP-1 cycle so that no unwanted Nitrogen magnetization survives in the transverse plane. To ensure complete z-rotation of the transverse component of Nitrogen magnetization, the decoupling schemes have been bracketed by two 90° pulses. For each scan, after the acquisition of the ^{13}C transient, a gradient is applied to kill any undesired magnetization and then the N_zC_z magnetization is transferred to $^{15}N_i$, $^{15}N_{i-1}$and $^{15}N_{i+1}$ by a 90° pulse on ^{15}N channel. This is followed by a second ^{15}N constant time evolution period (30 ms) including t_2. During this period the ^{15}N magnetization becomes in-phase with respect to $^{13}C^{\alpha}$ and antiphase with respect to its amide proton. Finally, the ^{15}N magnetization is transferred back to the amide proton by back INEPT and the proton magnetization is detected during the acquisition period t_3. The ^{13}CO spins are decoupled during both t_1 and t_2 periods by selective 180° pulses whose offsets were kept at 176 ppm. The magnetization transfer pathways for the entire experiment is summarized as follows

$$H_i \rightarrow N_i \rightarrow C_i^{\alpha}, C_{i-1}^{\alpha} \rightarrow N_i, N_{i-1}, N_{i+1} \rightarrow H_i, H_{i-1}, H_{i+1}$$
$$(t_1) \quad (t_2') \qquad (t_2) \qquad (t_3)$$

The 2D data set (t_1, t_2') generates the $^{13}C^{\alpha}$–^{15}N correlation spectrum which provides sequential connectivity between consecutive residues $i-1$ and i. The 3D data set (t_1, t_2, t_3) generates the standard 3D HNN experiment displaying $^{1}H^{N}$ and ^{15}N correlations between three

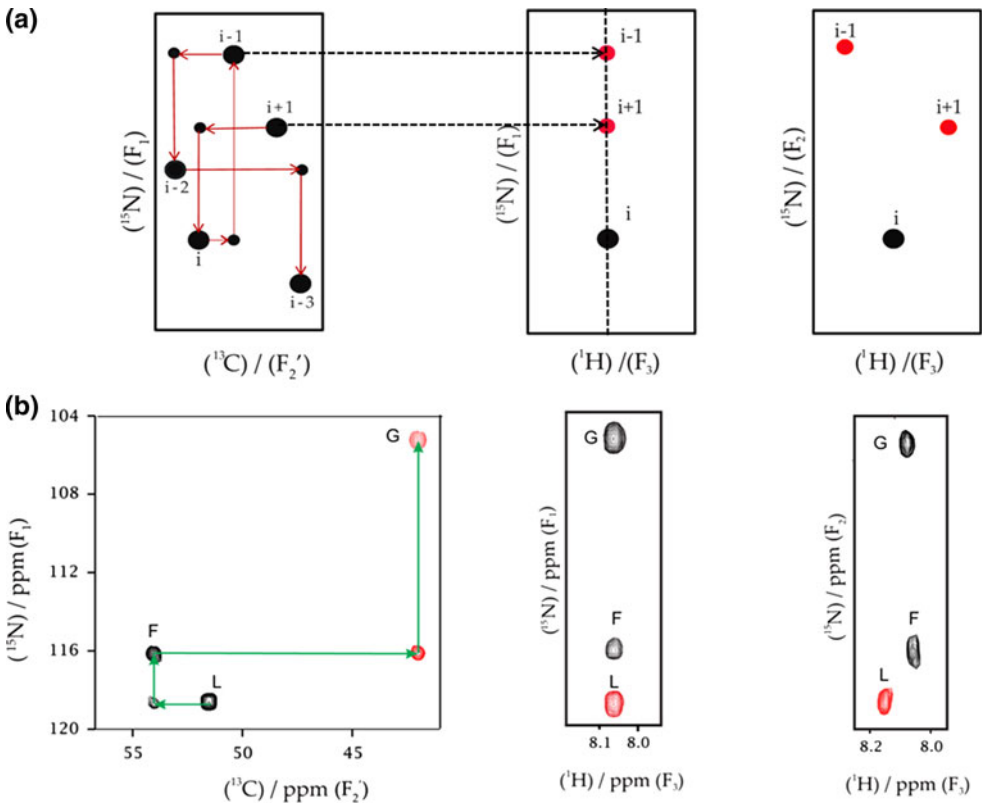

Fig. 3 **a** Schematic representation of 2D $^{13}C^{\alpha}$–^{15}N sequential correlations obtained along with 3D (^{15}N–^{15}N–^{1}H) correlations from the implementation of dual detection in HNN. The assignment protocol with $^{13}C^{\alpha}$–^{15}N (F_1–F_2') correlation spectrum, F_1–F_3 and F_2–F_3 planes of HNN is demonstrated. The self-peaks in the $^{13}C^{\alpha}$–^{15}N correlation spectrum are labeled and the connectivities to the sequential peaks are denoted by *solid arrows*. The correspondence of the $i-1$th and $i+1$th peaks in the planes of HNN are denoted by *dashed arrows*. The i, $i-1$ and $i+1$th peaks on the F_1–F_3 plane of HNN at H_i chemical shift are connected by a *dashed line*. **b** The $^{13}C^{\alpha}$–^{15}N correlation spectrum and F_1–F_3, F_2–F_3 planes of GFL at the N_i of Phe residue are shown for a simple demonstration of the above scheme. *Black* and *red* peaks represent positive and negative contours, respectively

consecutive residues, $i - 1$, i, and $i + 1$ on its different 2D planes and the peaks appear at the coordinates (Bhavesh et al. 2001):

$$F_1 = N_i,\ (F_2,\ F_3) = (H_i, N_i), (H_{i-1}, N_{i-1}), (H_{i+1}, N_{i+1})$$

$$F_2 = N_i,\ (F_1, F_3) = (H_i, N_i), (H_i, N_{i-1}), (H_i, N_{i+1})$$

The self peak, (H_i, N_i), is positive whereas the sequential peaks, (H_{i-1}, N_{i-1}), (H_{i+1}, N_{i+1}), are negative (Bhavesh et al. 2001) in both the planes.

The 2D $^{13}C^{\alpha}$–^{15}N sequential correlations obtained from this 3D experiment yield many-fold benefits. First, the Glycine peaks have negative signs while the rest are positive (Supporting information Fig. S1), and this serves as check point information during sequential walk. This is in contrast to the 2D $^{13}C^{\alpha}$–^{15}N correlation spectra reported earlier (Bermel et al. 2006). Second, the 2D $^{13}C^{\alpha}$–^{15}N correlation spectrum connects only the preceding residue and thereby provides directionality in the backbone walk with HNN, which otherwise requires a 3D HN(C)N (Bhavesh et al. 2001; Panchal et al. 2001). Third, for each residue-type, the range of chemical shift dispersion along both $^{13}C^{\alpha}$ and ^{15}N dimensions is wide, as is evident from Fig. 2 (also see Supporting Information, Fig. S2), which facilitates assignments in regions with poor ^{1}H chemical shift dispersion. The scheme of sequential walk as obtained by comparing the $^{13}C^{\alpha}$–^{15}N (F_1–F_2') correlation spectrum with the N–H^N correlations in the F_1–F_3 and F_1–F_2 planes of 3D HNN are schematically represented in Fig. 3a. We wish to point out here that the intensity of the ith peak is almost twice that of the $i - 1$th peak which helps in distinguishing the self peak from the preceding one at a particular ^{15}N chemical shift (detailed description is included in Supporting information, Fig. S1). The multiple-acquisition protocol was first tested on the standard (^{13}C, ^{15}N) labeled GFL sample. The different correlation spectra obtained on GFL from the inclusion of ^{13}C and ^{1}H detections are shown in Fig. 3b, where the extreme left hand block represents the $^{13}C^{\alpha}$–^{15}N correlation spectrum, whereas the middle and the right hand blocks represent the F_1–F_3 and F_2–F_3 cross-sections of HNN at the N_i of Phenylalanine (F) residue. The sequential connections are clearly easily discernible. It is important to point out here that incorporation of $^{13}C^{\alpha}$ acquisition did not affect the coherence transfer pathway of 3D HNN (Supplementary Information, Fig. S3). Next, the possibility of obtaining full assignments from the 2D $^{13}C^{\alpha}$–^{15}N correlation spectrum was tested on a (^{13}C, ^{15}N) labelled Ubiquitin sample (1.6 mM concentration). This spectrum recorded on an 800 MHz spectrometer equipped with cryogenically cooled probe with 64 scans with 1 increment in t_2 dimension is shown in Fig. 4 and the average signal-to-ratio of the cross-peaks in the spectrum is ~25. We were able to assign all

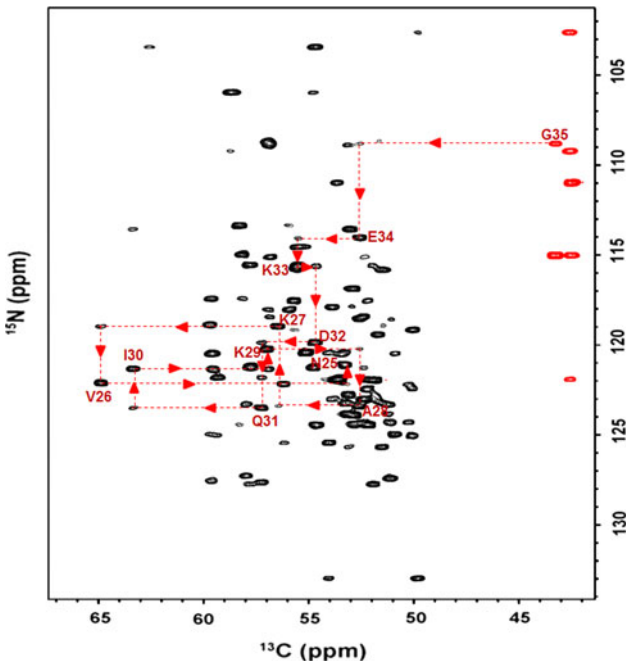

Fig. 4 Illustrative backward sequential walks along the polypeptide chain in the 2D $^{13}C^{\alpha}$–^{15}N correlation spectrum: the connectivities in the stretch of residues Gly35–Asn25 of ^{15}N,^{13}C labeled Ubiquitin are denoted by *dashed arrows* (*red*). The walk initiated from Glycine (Gly 35) and continued till we encountered a Proline (Pro 24). The spectrum was recorded on an 800 MHz spectrometer equipped with a cryogenically cooled probe

the peaks in the spectrum by backward walk along the polypeptide chain. As an illustration, the connectivities in the stretch of residues Gly35–Asn25 are denoted by dashed lines in the figure. The assignments of the peaks in the spectrum are indicated by residue label annotations in Fig. S4. We like to point out here that during $^{13}C^{\alpha}$ acquisition by the second receiver, Cα–CO (55 Hz) and Cα–Cβ (35 Hz) couplings are active and this would result in peak splittings. However due to short acquisition time (~20 ms) these would be unresolved but show up as line broadening. The splitting due to coupling can possibly be removed by inclusion of DIPAP (Bermel et al. 2005, 2006) in the pulse programme, but it will result in a loss of signal due to the addition of extra delays, so we have abstained from inclusion of this element.

We seriously considered the sensitivity of the new experiment in comparison with normal HNN. As mentioned earlier, in the normal HNN magnetization transfer pathway, the in-phase carbon magnetization generated at the end of 2τ period is discarded by dephasing by gradients while the desired magnetization is converted into C_ZN_Z before transferring it to transverse nitrogen magnetization. In the present modification, the discarded C^{α} magnetization is collected during the t_2' period and during this time the C_ZN_Z remains unchanged. Whatever relaxation happens for

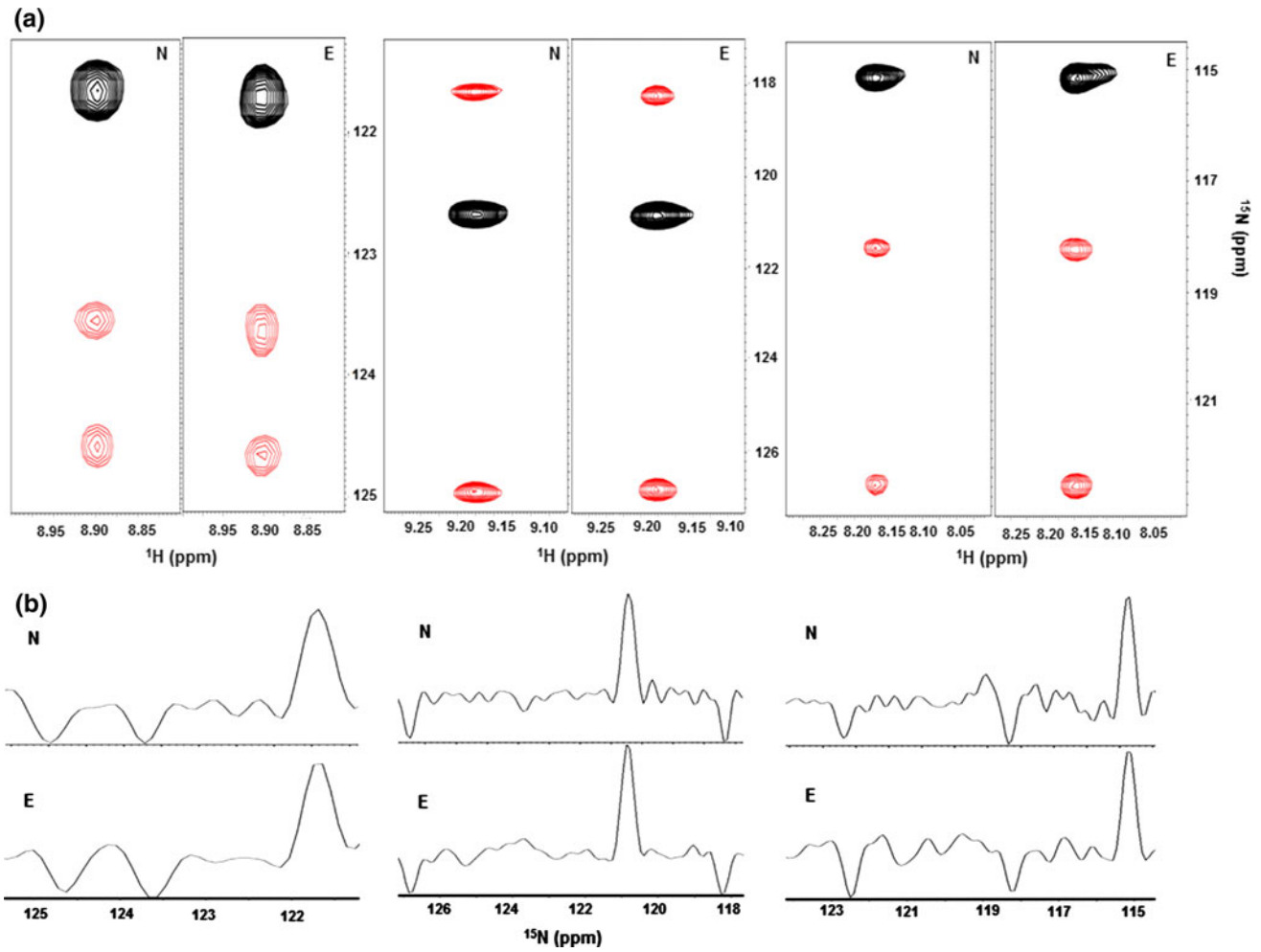

Fig. 5 Sensitivity comparison of normal HNN (N) and the extended version (E) with 16 scans on ^{15}N,^{13}C labeled Ubiquitin. **a** F_1–F_3 planes of Ubiquitin at $F_2 = 121.7$, 120.8 and 115.1 ppm obtained from N and E versions of HNN. **b** 1D traces obtained from the cross-section of the peaks along F_1 dimension. The noise level was kept identical in both the cases. The similar amplitudes of the signals indicate almost identical sensitivities of the two versions of the experiment. The total experimental times were approximately 17 h in normal HNN and 17 h 40 min in the modified HNN. Both the experiments were acquired with 1,024 × 24 × 136 complex points along F_3, F_2, F_1 dimensions with spectral widths of 12, 34 and 34 ppm, respectively

this term is the one that will contribute to the total loss of sensitivity in the spectrum. It is easy to see that 20 ms (t_2'max) is not such a long time for the ZZ order to relax. Moreover, we may mention that the replacement of the selective transfer pulse on C^{α} (200 μs) with a short hard pulse minimizes the relaxation loss during the pulse-length in the modified version. Thus we do not expect too much loss of sensitivity due to the modification in the HNN presented here. Indeed this is demonstrated in Fig. 5. As is evident, the sensitivities in the two experiments are almost identical.

To summarize, we have implemented dual receivers in the 3D HNN experiment and put to use the otherwise discarded $^{13}C^{\alpha}$ transverse magnetization. This has appended new informations from $^{13}C^{\alpha}$ to the HNN experiment by creating 2D $^{13}C^{\alpha}$–^{15}N sequential correlation spectrum along with characteristic Glycine specific check point information, and the standard 3D ^{15}N–^{15}N–^{1}H correlations. The former provides directionality to sequential walk in HNN, on one hand, and because of check point information and availability of high dispersion in $^{13}C^{\alpha}$–^{15}N chemical shift maps, removes any ambiguities in assignments, on the other. Hence, the detection of $^{13}C^{\alpha}$ and ^{1}H magnetizations within the same experiment has demonstrably enabled unambiguous assignment of a protein from a single experiment. We foresee that such implementations would provide new boosts to NMR applications in chemistry and biology, in general, in the coming future.

Acknowledgments We thank the Government of India for providing financial support to the National Facility for High Field NMR at TIFR. We like to express our sincere gratitude to Dr. P. K. Madhu for his critical suggestions.

References

Bermel W, Bertini I, Duma L, Felli IC, Emsley L, Pierattelli R, Vasos PR (2005) Complete assignment of heteronuclear protein resonances by protonless NMR spectroscopy. Angew Chemie 44:3089–3092

Bermel W, Bertini I, Felli IC, Piccioli M, Pierattelli R (2006) 13C-detected protonless NMR spectroscopy of proteins in solution. Prog Nucl Mag Res Sp 48:25–45

Bhavesh NS, Panchal SC, Hosur RV (2001) An efficient high-throughput resonance assignment procedure for structural genomics and protein folding research by NMR. Biochemistry 40:14727–14735

Emsley L, Bodenhausen G (1990) Gaussian pulse cascades: new analytical functions for rectangular selective inversion and in-phase excitation in NMR. Chem Phys Lett 165:469–476

Freeman R, Kupce E (2008) Molecular structure from a single NMR experiment. J Am Chem Soc 130:10788–10792

Freeman R, Kupce E (2010a) High-resolution NMR correlation experiments in a single measurement (HR-PANACEA). Magn Reson Chem 48:333–336

Freeman R, Kupce E (2010b) Molecular structure from a single NMR sequence (fast-PANACEA). J Magn Reson 206:147–153

Kupce E (2011) NMR with multiple receivers. Top Curr Chem. doi: 10.1007/128_2011_226

Kupce E, Wrackmeyer B (2010) Multiple receiver experiments for NMR spectroscopy of organosilicon compounds. Appl Organomet Chem 24:837–841

Kupce E, Freeman R, John BK (2006) Parallel acquisition of two-dimensional NMR spectra of several nuclear species. J Am Chem Soc 128:9606–9607

Kupce E, Kay LE, Freeman R (2010) Detecting the 'afterglow' of 13C NMR in proteins using multiple receivers. J Am Chem Soc 132:18008–18011

Marion D, Ikura M, Tschudin R, Bax A (1989) Rapid recording of 2D NMR spectra without phase cycling. Application to the study of hydrogen exchange in proteins. J Magn Reson 85:393–399

Panchal SC, Bhavesh NS, Hosur RV (2001) Improved 3D triple resonance experiments, HNN and HN(C)N, for HN and 15 N sequential correlations in (13C, 15N) labeled proteins: application to unfolded proteins. J Biomol NMR 20:135–147

Shaka AJ, Keeler J, Freeman R (1983a) Evaluation of a new broadband decoupling sequence: WALTZ-16. J Magn Reson 53:313–349

Shaka AJ, Keeler J, Frenkiel T, Freeman R (1983b) An improved sequence for broadband decoupling: WALTZ-16. J Magn Reson 52:335–338

Shaka AJ, Barker PB, Freeman R (1985) Computer-optimized decoupling scheme for wideband applications and low-level operation. J Magn Reson 64:547–552